

**DESCRIPTION AND UNIQUE CRYSTAL-STRUCTURE OF WATERHOUSEITE,
A NEW HYDROXY MANGANESE PHOSPHATE SPECIES FROM THE IRON
MONARCH DEPOSIT, MIDDLEBACK RANGES, SOUTH AUSTRALIA**

ALLAN PRING[§]

*Department of Mineralogy, South Australian Museum, North Terrace, Adelaide, South Australia 5000,
and School of Earth & Environmental Science, University of Adelaide, Adelaide, S.A. 5005, Australia*

UWE KOLITSCH

Institut für Mineralogie und Kristallographie, Geozentrum, Universität Wien, Althanstr. 14, A-1090 Wien, Austria

WILLIAM D. BIRCH

Department of Mineralogy, Museum of Victoria, GPO Box 666E, Melbourne, Victoria, 3000, Australia

ABSTRACT

Waterhouseite from the Iron Monarch mine, Iron Knob, South Australia, is a new hydroxy manganese phosphate species that has a unique crystal-structure. The mineral was found in a carbonate-rich zone with gatehouseite, seamanite, rhodochrosite, shigaite, barite, hausmannite and hematite. It occurs as divergent sprays of orange-brown to dark brown bladed crystals up to 1 mm in length but only up to 20 μm in thickness. The crystals are transparent with a pearly luster on cleavages, but it is vitreous to pearly on the tabular faces. The mineral is brittle, with a conchoidal fracture and a yellowish brown streak. There is a perfect cleavage on (100) and a probable cleavage on (001). The crystals show the principal forms {100} (dominant), {010}, {011} and {001}. All crystals are twinned on (100) by non-merohedry. The Mohs hardness is estimated to be ~4, and the measured density is 3.55(5) g/cm^3 (calculated density is 3.591 g/cm^3). Crystals are biaxial negative and length-slow, with α 1.730(3), β ~1.738 and γ 1.738(4), but $2V$ could not be measured. Interference colors are normal, implying the absence of optical dispersion. The optical orientation is $XYZ = bac$ (pseudo-orthorhombic), and the pleochroism is X pale brownish, Y brown-yellow, Z pale brownish, with absorption $Z = X > Y$. Electron-microprobe analyses yielded the empirical formula $\text{Mn}_{7.29}(\text{P}_{1.81}\text{As}_{0.07}\text{V}_{0.04})_{\Sigma 1.92}\text{O}_{7.68}(\text{OH},\text{O})_{8.32}$, calculated on the basis of 16 O atoms. The simplified formula is $\text{Mn}_7(\text{PO}_4)_2(\text{OH})_8$, in agreement with the crystal-structure determination. The strongest five lines in the powder X-ray-diffraction pattern [d in \AA (I)(hkl)] are: 4.436(70)(111), 3.621(100)(202), 3.069(50)(311), 2.941(40)(013), and 2.780(35)(020). Unit-cell parameters refined from powder-diffraction data, a 11.364(6), b 5.570(2), c 10.455(3) \AA , β 96.61(3) $^\circ$, V 657.4(2) \AA^3 ($Z = 2$), agree very well with those refined from the single-crystal data. The crystal structure was solved by direct methods and refined in space group $P2_1/c$ to $R1(F) = 5.15\%$ and $wR2_{\text{all}}(F^2) = 16.28\%$ using data from a twinned crystal (by non-merohedry) with 1400 "observed" reflections with $F_o > 4\sigma(F_o)$. The crystal structure is characterized by a dense, complex framework of $\text{Mn}(\text{O},\text{OH})_6$ octahedra and PO_4 tetrahedra, which are linked by both edges and corners. Two different subunits can be recognized in the structure: arsenoclasite-type strips of edge-sharing octahedra (fragments of brucite-pyrochroite-type sheets of octahedra) and finite chains of edge-sharing octahedra (fragments of infinite rutile-type chains). The PO_4 tetrahedra provide a connection between the strips and the chains. Single-crystal Raman spectra confirm weak hydrogen bonding. A unique feature of the structure is that the single PO_4 tetrahedron shares two of its edges with $\text{Mn}(\text{O},\text{OH})_6$ octahedra. Only two synthetic anhydrous metal arsenates are known that show a corresponding sharing of two edges. The structure of waterhouseite has no equivalent, although the unit-cell parameters reveal some relations with the two chemical analogues allactite, $\text{Mn}_7(\text{AsO}_4)_2(\text{OH})_8$, and raadeite, $\text{Mg}_7(\text{PO}_4)_2(\text{OH})_8$.

Keywords: new mineral species, waterhouseite, manganese phosphate, crystal structure, Iron Monarch mine, Australia.

SOMMAIRE

La waterhouseïte, nouvelle espèce de phosphate de manganèse hydroxylé découverte à la mine Iron Monarch, à Iron Knob, en Australie du Sud, possède une structure cristalline très inhabituelle. Elle a été découverte dans une zone carbonatée associée à gatehouseïte, seamanite, rhodochrosite, shigaïte, barite, hausmannite et hématite. Elle se présente en amas divergents de cristaux en lames orange-brun à brun foncé, atteignant 1 mm en longueur mais seulement 20 μm en épaisseur. Les cristaux sont transpar-

[§] E-mail address: pring.allan@saugov.sa.gov.au

ents, avec un éclat nacré sur les clivages, mais plutôt vitreux à nacré sur les faces des cristaux. Le minéral est cassant, à fracture conchoïdale, et à rayure brun jaunâtre. Il y a un clivage parfait sur (100) et un clivage probable sur (001). Les cristaux montrent les formes principales {100} (dominante), {010}, {011} et {001}. Tous les cristaux sont maclés sur (100) par non-mérodrie. La dureté de Mohs serait environ 4, et la densité mesurée est $3.55(5) \text{ g/cm}^3$ (la densité calculée est 3.591 g/cm^3). Les cristaux sont biaxes négatifs et à allongement négatif, avec $\alpha 1.730(3)$, $\beta \sim 1.738$ et $\gamma 1.738(4)$, mais nous n'avons pas pu mesurer l'angle $2V$. Les couleurs d'interférence sont normales, ce qui implique l'absence de dispersion optique. L'orientation optique est $XYZ = bac$ (pseudo-orthorhombique), et le pléochroïsme est: X brun pâle, Y brun-jaune, Z brun pâle, avec absorption $Z = X > Y$. Les analyses effectuées avec une microsonde électronique ont mené à la formule empirique $\text{Mn}_{7.29}(\text{P}_{1.81}\text{As}_{0.07}\text{V}_{0.04})_{\Sigma 1.92}\text{O}_{7.68}(\text{OH},\text{O})_{8.32}$, calculée sur une base de seize atomes d'oxygène. La formule simplifiée serait $\text{Mn}_7(\text{PO}_4)_2(\text{OH})_8$, en accord avec les résultats de l'ébauche de la détermination de la structure. Les cinq raies les plus intenses du spectre de diffraction X (méthode des poudres) [d en Å(hkl)] sont: $4.436(70)(111)$, $3.621(100)(202)$, $3.069(50)(311)$, $2.941(40)(013)$, et $2.780(35)(020)$. Les paramètres réticulaires affinés à partir des données acquises sur poudre, $a 11.364(6)$, $b 5.570(2)$, $c 10.455(3)$ Å, $\beta 96.61(3)^\circ$, $V 657.4(2)$ Å³ ($Z = 2$), concordent très bien avec celles qui résultent de l'affinement sur monocristal. Nous avons résolu la structure par méthodes directes, et nous l'avons affiné dans le groupe spatial $P2_1/c$ jusqu'à un résidu $R1(F)$ de 5.15% [$wR2_{\text{toutes}}(F^2) = 16.28\%$] en utilisant les données obtenues d'un cristal maclé (par non-mérodrie), et les 1400 réflexions "observées" ayant $F_o > 4\sigma(F_o)$. La structure possède une trame dense d'octaèdres $\text{Mn}(\text{O},\text{OH})_6$ et de tétraèdres PO_4 , qui sont liés à la fois par partage d'arêtes et de coins. La structure contient deux sous-unités: il y a des rubans d'octaèdres à arêtes partagées, comme dans l'arsénoclasite (des fragments de feuillets d'octaèdres comme dans la brucite ou la pyrochroïte) et des chaînes finies d'octaèdres à arêtes partagées (des fragments de chaînes infinies comme dans le rutile). Les tétraèdres PO_4 assurent une connexion entre les rubans et les chaînes. Les spectres de Raman obtenus sur monocristaux confirment la présence de faibles liaisons hydrogène. Un aspect unique de la structure concerne le tétraèdre PO_4 , qui partage deux de ses arêtes avec des octaèdres $\text{Mn}(\text{O},\text{OH})_6$. Ce partage inhabituel n'est connu que dans deux arsenates anhydres synthétiques. La structure de la waterhouseïte n'a aucun équivalent, quoique les paramètres réticulaires révèlent certains liens avec les analogues du point de vue chimique, allactite, $\text{Mn}_7(\text{AsO}_4)_2(\text{OH})_8$, et raadeïte, $\text{Mg}_7(\text{PO}_4)_2(\text{OH})_8$.

Mots-clés: nouvelle espèce minérale, waterhouseïte, phosphate de manganèse, structure cristalline, mine Iron Monarch, Australie.

INTRODUCTION

The Iron Monarch mine, a Precambrian sedimentary iron ore deposit in the Middleback Ranges, at Iron Knob, South Australia, is one of the most productive sources of rare and unusual mineral species in Australia. Broken Hill Proprietary Limited worked the mine as a source of high-grade iron ore for many years. In May 1987, Mr Glyn Francis, then a Quality Control Officer at the mine, submitted a group of specimens to one of the authors (AP) for identification. One of the specimens contained some small clusters of very small and thin brownish, blade-like crystals which energy-dispersion X-ray analysis showed to contain manganese, phosphorus and a minor amount of arsenic. The powder X-ray-diffraction pattern could not be matched to any known mineral, although similarities were noted to a number of manganese arsenate minerals, including allactite ($\text{Mn}_7(\text{AsO}_4)_2(\text{OH})_8$). Although Mr. Francis was able to locate several more small specimens containing the mineral, there was still insufficient material for a full characterization. Only the later crystal-structure determination from data collected on a modern single-crystal diffractometer equipped with a CCD area detector led to a complete characterization of this mineral. The new species has been named waterhouseïte in honor of Frederick George Waterhouse (1815–1898), naturalist and first Director of the South Australian Museum (Adelaide), in recognition of his contribution to the preservation of the natural history of South Australia. Waterhouse was the youngest brother of George Robert

Waterhouse (1810–1888), who was Keeper of Geology at the British Museum (London) from 1845 until 1880. The name also celebrates the continuing work of the Waterhouse Club in their support of the South Australian Museum. The mineral and the name were unanimously approved by the IMA Commission on New Minerals and Mineral Names (no. 2004–035). The type specimen and additional material are held in the collections of the South Australian Museum, Adelaide (SAM 28408 and 28409).

OCCURRENCE

The Iron Monarch deposit ($32^\circ 45' \text{S}$, $137^\circ 08' \text{E}$) is the largest of a number of Precambrian sedimentary iron ore deposits in the Middleback Ranges of South Australia, some 500 km northwest of Adelaide. The Middleback Ranges are composed primarily of a sequence of Early Proterozoic chemical metasediments (the Middleback Group), which are interpreted to have been deposited about 1950 to 1850 million years ago (Yeates 1990). The orebody lies within a carbonate-facies iron formation, composed primarily of iron carbonate, silica and iron oxide, with primary iron silicates such as iron-rich talc and cummingtonite–grunerite. Hematite and quartz become predominant at the top of the sequence and constitute the orebody. There appear to have been at least two periods of mobilization of iron-rich fluids, the first being in the Middle Proterozoic and the second during a period of intense weathering in the Tertiary (Miles 1955, Yeates 1990). The extensive suite of

secondary phosphate and other oxysalt minerals appears to have been formed as a result of deep Tertiary and post-Tertiary weathering of the deposit.

The new mineral occurs in cavities in a matrix consisting of hematite, hausmannite, barite, manganian calcite and rhodochrosite, from the 130-meter level on the eastern side of the Iron Monarch open cut. Shigaite, gatehouseite, seamanite, rhodochrosite, barite, hausmannite and hematite are found in close association with waterhouseite. Metaswitzerite, sussexite, arsenoclasite, collinsite, pyrobelonite, triploidite and a new, unnamed hexagonal calcium–manganese carbonate–phosphate have also been noted on specimens from the same immediate area of the open cut, but not in direct association with waterhouseite (Pring *et al.* 1989, 1990, 1992a, b, 2000, Pring & Birch 1993). Mining operations ceased at Iron Monarch in April 1998, and the mine site has been partially rehabilitated. Unfortunately, it is no longer accessible for collecting. To date, over 140 mineral species have been identified from this locality. Pring *et al.* (2000) provided a full list. Waterhouseite was noted in Pring *et al.* (2000) as an unidentified phase designated UK02.

PHYSICAL AND OPTICAL PROPERTIES

Waterhouseite occurs as divergent sprays of bladed crystals up to $1.0 \times 0.2 \times 0.02$ mm with an elongation parallel to [001] (Fig. 1). The principal forms observed are {100} (dominant), {010}, {011} and {001} (not on all crystals); if {001} is missing, a spear-shaped

outline of the blades results, and the angle enclosed by the left and right boundary faces of the flat “spear tip” is $18 \pm 1^\circ$. Single-crystal studies provide evidence that the mineral invariably shows contact twinning (by non-merohedry) on the platy face (100). If a bladed twin crystal is seen edge-on under the polarizing microscope, the twinning may be recognizable from a strongly re-entrant angle between two twin individuals. The crystals have splintery to conchoidal fracture, with a perfect cleavage on (100) and a probable cleavage on (001). Waterhouseite is transparent, and the color ranges from resinous orange-brown to dark clove-brown with a yellowish brown streak. The luster is pearly on cleavages and vitreous to pearly on crystal faces, and the Mohs hardness is estimated to be 4. The density was measured to be $3.55(5)$ g/cm³ by suspension in a mixture of Clerici solution and water, whereas the calculated density (with $Z = 2$) is 3.591 g/cm³, based on the chemical formula derived from the structure refinement, and 3.49 g/cm³ based on the simplified formula, $\text{Mn}_7(\text{PO}_4)_2(\text{OH})_8$.

Optically, waterhouseite is biaxial negative and length-slow, with α 1.730(3), β \sim 1.738 and γ 1.738(4) (measured in white light). The optic angle could not be measured, but it must be small because β is very close to γ . Interference colors are normal, implying absence of optical dispersion. The optical orientation is $XYZ = bac$ (pseudo-orthorhombic), and the pleochroism is X pale brownish, Y brown-yellow, Z pale brownish, with absorption $Z = X > Y$.

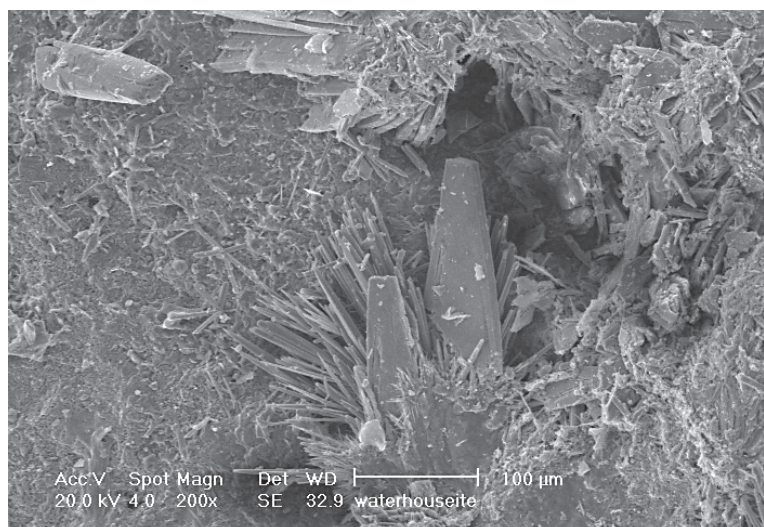


FIG. 1. SEM micrograph of waterhouseite showing the blade-like habit of the crystals. The crystals show the principal forms {100} (dominant), {010}, {011}, and {001}.

CHEMICAL AND POWDER-DIFFRACTION DATA

The chemical composition of waterhouseite was established using a Cameca SX50 electron microprobe, at 15 kV and a specimen current of about 20 nA. We used pure metals (Mn, V and Cu), wollastonite (Ca), hematite (Fe), corundum (Al), fluorapatite (P), sphalerite (Zn) and arsenopyrite (As) as standards. Electron-microprobe analysis showed that the mineral is essentially a pure manganese phosphate with minor substitution of arsenic for phosphorus, traces of Al and Zn, and variable, very minor amounts of Si, but gave consistently low and somewhat variable totals (80 to 84 wt.% without H₂O). No other elements with $Z > 9$ were detected during a wavelength-dispersion scan; Mg was sought specifically but not found. Raman spectroscopy (see below) showed no carbonate or borate groups. There was insufficient material to determine H₂O directly, so the amount was calculated from the crystal-structure determination, which gave the ideal formula Mn₇(PO₄)₂(OH)₈ (see below). Further probe mounts were made (five grains in all), but the analytical total remained low. It was noted, however, that the crystal fragments were very thin. We conclude that the low totals were mostly due to part of the electron beam passing through the crystals into the resin matrix. The analytical results were thus normalized to the ideal Mn content, and the H₂O calculated to give eight OH groups. Seven analyses were made from multiple crystals, with the calculated oxide averages and ranges shown in Table 1. These results demonstrate that there is only very limited substitution of As and V for P. The empirical formula, calculated on the basis of 16 O atoms, as shown by the crystal structure, is Mn_{7.29}[(P_{1.81}As_{0.07}V_{0.04})Σ_{1.92}O_{7.68}](OH, O)_{8.32}, and the simplified formula is Mn₇(PO₄)₂(OH)₈. The empirical formula shows an excess of Mn and a deficit in the P site; we believe that this may be partly due to small but variable amounts of Si-for-P substitution (rarely up to 2.5 wt% SiO₂) that could not be reproducibly established. The Gladstone–Dale compatibility index is 0.010, indicating “superior” agreement between the chemical and physical data (Mandarino 1981).

TABLE 1. ELECTRON-MICROPROBE DATA FOR WATERHOUSEITE

| Constituent | wt. % | Range | Probe standard |
|--------------------------------|-------|---------------|----------------|
| MnO | 69.70 | 69.15 – 71.45 | Mn metal |
| ZnO | 0.02 | 0.0 – 0.07 | sphalerite |
| P ₂ O ₅ | 17.37 | 16.46 – 18.53 | fluorapatite |
| As ₂ O ₃ | 1.09 | 0.41 – 2.31 | arsenopyrite |
| V ₂ O ₅ | 0.50 | 0.0 – 0.91 | V metal |
| H ₂ O (calc.)* | 9.49 | | |
| TOTAL | 98.36 | | |

Note: number of analyses made: 7. * From structure solution. The empirical formula, Mn_{7.29}[(P_{1.81}As_{0.07}V_{0.04})O₄]_{Σ1.92}(OH, O)_{8.32}, is based on 16 atoms of oxygen.

Powder X-ray-diffraction data for waterhouseite (Table 2) were obtained using a Guinier–Hägg camera 100 mm in diameter, CrK α radiation (λ 2.28970 Å) and silicon (NBS SRM 640a) as an internal standard. The Guinier–Hägg films were scanned in *TPU/Pos* mode using an Epson film scanner, and the powder-diffraction profile over the 2θ range 10 to 90° was extracted using the program SCION IMAGE and the Universal-Si-Calibration, a macro function based on IGOR PRO 4.0 (WaveMetrics Inc., 2000). The unit-cell parameters were refined by treating the whole powder pattern with the Le Bail profile-fitting method (Le Bail *et al.* 1988), starting from the unit-cell parameters measured with single-crystal techniques. The final unit-cell parameters, a 11.364(6), b 5.570(2), c 10.455(3) Å, β 96.61(3)°, V 657.4(2) Å³, are very similar to those obtained from the single-crystal refinement of the structure (see below). The axial ratios calculated from these cell parameters are 2.0402:1:1.8770.

RAMAN SPECTROSCOPY

Single-crystal laser-Raman spectra of waterhouseite (Fig. 2) were recorded in the range from 3800 to 100 cm⁻¹ with a Renishaw Ramascope 1000 using a laser wavelength of 518 nm (green laser) and excitation through a Leica DMLM optical microscope (Si standard, spectral resolution ± 4 cm⁻¹, minimum lateral resolution ~ 2 mm, unpolarized laser light, random sample orientation). Very similar spectra were recorded with a blue laser (488 nm) on a Renishaw M1000 MicroRaman Imaging System in Vienna, but they are of poorer quality (strong background that increases toward higher wavenumbers, and relatively low intensity of all bands), and therefore are not shown here. The spectrum obtained with the green laser (Fig. 2) shows two medium strong bands due to O–H stretching vibrations at 3439 and 3510 cm⁻¹, and two shoulders at

TABLE 2. POWDER X-RAY-DIFFRACTION DATA FOR WATERHOUSEITE

| hkl | d_{obs} | d_{calc} | h | k | l | hkl | d_{obs} | d_{calc} | h | k | l |
|-------|-----------|------------|-----|-----|-----------|-------|-----------|------------|-----|-----|-----------|
| 15 | 4.980 | 4.995 | 1 | 1 | 0 | 35 | 2.780 | 2.785 | 0 | 2 | 0 |
| 5 | 4.613 | 4.594 | 1 | 1 | $\bar{1}$ | 20 | 2.718 | 2.719 | 2 | 1 | 3 |
| 70 | 4.436 | 4.415 | 1 | 1 | 1 | 10 | 2.691 | 2.690 | 0 | 2 | $\bar{1}$ |
| 15 | 3.811 | 3.808 | 2 | 1 | $\bar{1}$ | 10 | 2.610 | 2.609 | 4 | 0 | $\bar{2}$ |
| | | 3.798 | 0 | 1 | $\bar{2}$ | | | 2.600 | 1 | 2 | 1 |
| 5 | 3.763 | 3.763 | 3 | 0 | 0 | 20 | 2.596 | 2.596 | 0 | 0 | $\bar{4}$ |
| 100 | 3.621 | 3.619 | 2 | 0 | 2 | 10 | 2.496 | 2.506 | 4 | 1 | $\bar{1}$ |
| 15 | 3.283 | 3.283 | 2 | 0 | $\bar{2}$ | | | 2.498 | 2 | 2 | 0 |
| 50 | 3.069 | 3.067 | 3 | 1 | $\bar{1}$ | 15 | 2.469 | 2.469 | 2 | 0 | $\bar{4}$ |
| 5 | 3.037 | 3.035 | 2 | 1 | 2 | | | 2.469 | 1 | 0 | 4 |
| 40 | 2.941 | 2.940 | 0 | 1 | $\bar{3}$ | 10 | 2.399 | 2.401 | 2 | 2 | 1 |
| 20 | 2.890 | 2.893 | 3 | 0 | 2 | 10 | 2.371 | 2.372 | 1 | 2 | 2 |
| 20 | 2.842 | 2.822 | 4 | 0 | 0 | 10 | 2.363 | 2.363 | 4 | 1 | $\bar{2}$ |
| | | | | | | 10 | 2.353 | 2.353 | 0 | 1 | $\bar{4}$ |

Note: The indexing based on intensities calculated from the results of the structure determination. Refined unit-cell parameters: a 11.364(6), b 5.570(2), c 10.455(3) Å, β 96.61(2)°, V 657.4(2) Å³.

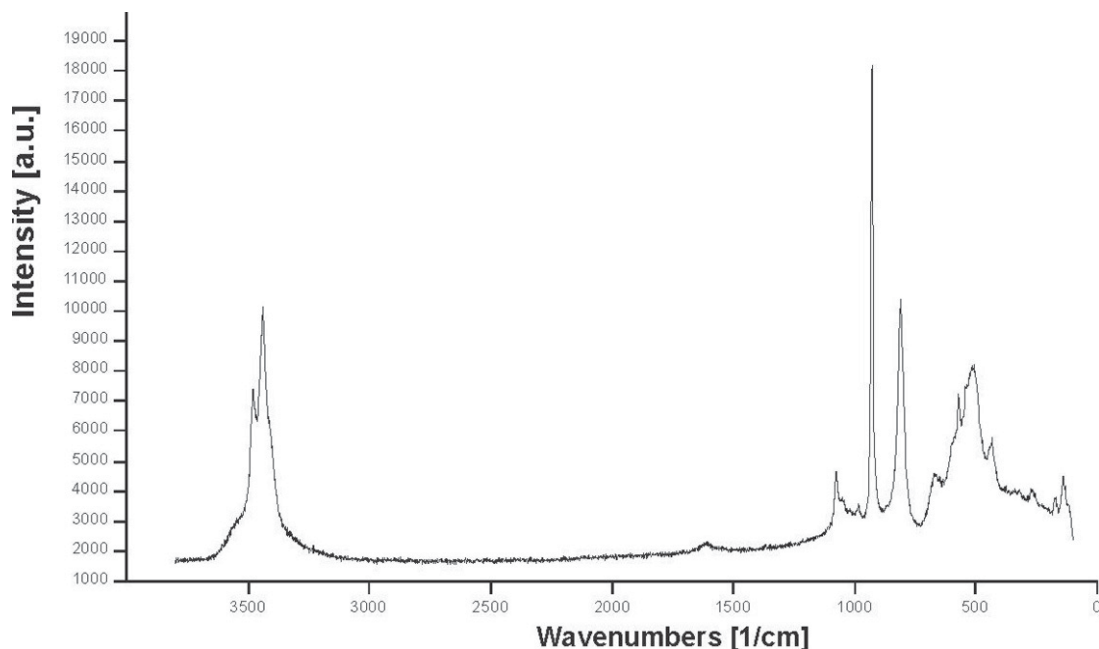


FIG. 2. Single-crystal laser-Raman spectra of waterhouseite. See text for discussion.

~ 3411 and ~ 3555 cm^{-1} . The existence of these bands agrees with the presence of four different OH groups in the structure. From the measured O–H band positions, OH–H...O distances between about 2.8 and 3.0 Å can be calculated using the correlation established by Libowitzky (1999); these distances would correspond to the weak hydrogen bonds provided by the four OH groups (OH...O distances between 2.89 and 3.12 Å, *vide infra*). A very weak, broad peak at ~ 1612 cm^{-1} could indicate the presence of impurities of molecular water (H–O–H bending mode), although it must be pointed out that Raman spectroscopy is not very sensitive for the detection of H₂O-bending modes; this peak could also represent an overtone of the band at 809 cm^{-1} . Below 1100 cm^{-1} , there is a group of very strong to very weak bands (the strong ones are italicized; sh: shoulder) *1076*, ~ 1050 , ~ 1018 , 984, *929*, *809*, 667, ~ 595 (sh), *571*, ~ 540 (sh), ~ 513 and 433 cm^{-1} , characteristic of vibrational modes of a PO₄ tetrahedron in a low-symmetry environment (all four fundamental PO₄ vibrations are Raman active). Lattice modes, including vibrations of Mn–O bonds, cause most of the strongly overlapping, weak bands below 400 cm^{-1} (~ 342 , ~ 321 , ~ 267 , 174 and ~ 137 cm^{-1}). A strong overlap could occur in the 500–400 cm^{-1} region between the bands attributed to vibrations of the PO₄ tetrahedron and of the Mn–O bonds (see Hatert *et al.* 2003, 2005). Accurate band-assignments are difficult owing to the low symmetry

of waterhouseite and the low site-symmetries of nearly all its atom positions.

CRYSTAL-STRUCTURE DETERMINATION

Single-crystal studies were done with a Nonius Kappa CCD four-circle diffractometer (MoK α radiation, CCD area detector) at 293 K. All waterhouseite crystals studied were found to be twinned by non-merohedry, with the twin plane parallel to the dominant face of the platy crystal (100). The crystal structure has been determined using a nearly full sphere of single-crystal intensity data collected from a twinned crystal; see Table 3 for experimental details. A large detector–crystal distance (40 mm) was chosen in order to avoid reflection overlap as much as possible. The structure was solved by direct methods (SHELXS97; Sheldrick 1997a) and refined, using SHELXL97 (Sheldrick 1997b), in space group *P2₁/c* (no. 14) to a preliminary *R1(F)* of about 12%. The structure model obtained corresponds to the chemical formula Mn₇(PO₄)₂(OH)₈, in agreement with the idealized formula derived from the chemical data. Hydrogen atoms could not be located owing to the effects of the twinning by non-merohedry. A total of 153 reflections most strongly affected by this twinning (reflections with $F_o \gg F_c$) were omitted during the final steps of the refinement, which caused *R1(F)* to drop from about 12% to about 5.5%. Final residuals

were $R1(F) = 5.15\%$ and $wR2_{\text{all}}(F^2) = 16.28\%$ [1400 "observed" reflections with $F_o > 4\sigma(F_o)$]. Before the final cycles of refinement, the atom coordinates were standardized using the program STRUCTURE TIDY (Gelato & Parthé 1987). Refined unit-cell parameters of the measured twin, a 11.364(2), b 5.569(1), c 10.455(2) Å, β 96.61(3)°, V 657.3(2) Å³, are basically identical with those calculated from the X-ray powder-diffraction data (Table 2). Atom coordinates and selected bond-lengths and angles (including probable hydrogen bonds) are given in Tables 4 and 5, respectively. A bond-valence

analysis for waterhouseite is presented in Table 6. A table of structure factors is available from the Depository of Unpublished Data, CISTI, National Research Council, Ottawa, Ontario K1A 0S2, Canada.

DESCRIPTION OF THE STRUCTURE

The asymmetric unit of waterhouseite contains four non-equivalent Mn atoms, one P atom, eight O atoms (four of which represent OH groups) and four H atoms; the latter were not detectable owing to the effects of twinning. The crystal structure is characterized by a dense, complex framework of Mn(O,OH)₆ octahedra and PO₄ tetrahedra, which are linked by both edges and corners (Figs. 3, 4). The framework is built of two types of subunits based on the Mn(O,OH)₆ octahedra: firstly, there are strips of edge-sharing octahedra built from Mn1O₂(OH)₄ and Mn4O₂(OH)₄ octahedra. Topologically identical strips occur in arsenoclasite and can be visualized as fragments of brucite–pyrochroite-type sheets of octahedra. The plane of these strips of octahedra is parallel to (102), and they extend along [010] (Fig. 3). A single strip is connected to two adjacent

TABLE 3. CRYSTAL DATA, DATA COLLECTION INFORMATION AND REFINEMENT DETAILS FOR WATERHOUSEITE

| Crystal data | | | |
|---|---|-------------------------------------|-------------------------------|
| Formula | Mn ₇ (PO ₄) ₂ (OH) ₈ | Formula weight | 710.58 |
| Space group | $P2_1/c$ (no. 14) | Z | 2 |
| a, b, c (Å) | 11.364(2), 5.570(1), 10.455(2) | | |
| β (°) | 96.61(3) | V (Å ³) | 657.3(2) |
| $F(000)$, ρ_{calc} (g·cm ⁻³) | 682, 3.591 | μ (mm ⁻¹) | 6.84 |
| Absorption correction [§] | multi-scan | | |
| Crystal dimensions (mm) | 0.02 × 0.05 × 0.10 | | |
| Data Collection | | | |
| Diffractometer | Nonius Kappa CCD system | | |
| λ (MoK α) (Å) | 0.71073, | T (K) | 293 |
| Crystal–detector dist. (mm) | 40 | Rotation axis, width (°) | φ, ω ; 1 |
| Total number of frames | 692 | Collection time per degree (s) | 289 |
| Collection mode, $2\theta_{\text{max}}$ (°) | 90% of Ewald sphere, 60 | | |
| h, k, l ranges | -15 - 15, -7 - 7, -14 - 14 | | |
| Total reflections measured | 3259 | Unique reflections | 1735 (R_{int} 2.4%) |
| Refinement | | | |
| Refinement on | F^2 | $R1(F)$, $wR2_{\text{all}}(F^2)^*$ | 5.15, 16.28% |
| "Observed" reflections | 1400 [$F_o > 4\sigma(F_o)$] | | |
| Extinction coefficient | 0.0012(13) | Number of refined parameters | 117 |
| GoodF | 1.037 | (D/s) _{max} | 0.0001 |
| Dr_{min} , Dr_{max} (e/Å ³) | -0.91, 2.12 | | |

** Note: Unit-cell parameters were refined from 1947 recorded reflections. Scattering factors for neutral atoms were employed in the refinement.

* $w = 1/[\sigma^2(F_o^2) + (0.1P)^2 + 5.1P]$; $P = ([\max(0, F_o^2)] + 2F_c^2) / 3$.

** The maximum positive peaks in the final difference-Fourier are considered to represent artifacts due to the twinning by nonmerohedry.

§ Otwinowski & Minor (1997), Otwinowski *et al.* (2003).

TABLE 4a. FRACTIONAL COORDINATES AND DISPLACEMENT PARAMETERS (Å²) OF ATOMS IN WATERHOUSEITE

| Atom | x | y | z | U_{eq} |
|------|-------------|-------------|-------------|-----------------|
| Mn1 | ½ | 0 | ½ | 0.0121(3) |
| Mn2 | 0.04797(9) | 0.53843(18) | 0.36737(10) | 0.0147(3) |
| Mn3 | 0.18562(9) | 0.51473(16) | 0.10420(10) | 0.0132(3) |
| Mn4 | 0.42873(9) | 0.00344(15) | 0.14595(9) | 0.0133(3) |
| P | 0.27486(13) | 0.3048(3) | 0.35133(14) | 0.0099(3) |
| O1 | 0.2819(4) | 0.1883(8) | 0.2186(4) | 0.0156(9) |
| O2 | 0.1796(4) | 0.1845(9) | 0.4256(4) | 0.0177(9) |
| O3 | 0.3986(4) | 0.3147(8) | 0.4344(4) | 0.0156(9) |
| O4 | 0.2326(4) | 0.5696(8) | 0.3215(4) | 0.0157(9) |
| Oh5 | 0.3432(4) | 0.6954(8) | 0.0569(4) | 0.0144(9) |
| Oh6 | 0.5401(4) | 0.3039(8) | 0.1800(4) | 0.0152(9) |
| Oh7 | 0.0206(4) | 0.3925(8) | 0.1718(4) | 0.0154(9) |
| Oh8 | 0.1019(4) | 0.6346(8) | 0.5682(4) | 0.0158(9) |

TABLE 4b. ANISOTROPIC DISPLACEMENT PARAMETERS (Å²) OF ATOMS IN WATERHOUSEITE

| Atom | U_{11} | U_{22} | U_{33} | U_{23} | U_{13} | U_{12} |
|------|-----------|------------|-----------|-------------|-------------|-------------|
| Mn1 | 0.0126(7) | 0.0114(6) | 0.0124(6) | -0.0002(4) | 0.0018(5) | 0.0004(4) |
| Mn2 | 0.0143(5) | 0.0161(4) | 0.0143(5) | -0.0016(3) | 0.0037(4) | -0.0014(3) |
| Mn3 | 0.0130(5) | 0.0137(5) | 0.0130(5) | 0.0006(3) | 0.0019(4) | -0.0004(3) |
| Mn4 | 0.0153(5) | 0.0115(5) | 0.0132(5) | -0.0002(3) | 0.0018(4) | -0.0012(3) |
| P | 0.0082(7) | 0.0114(6) | 0.0100(7) | 0.0000(5) | 0.0002(5) | 0.0010(5) |
| O1 | 0.012(2) | 0.019(2) | 0.015(2) | -0.0008(18) | 0.0005(16) | 0.0019(17) |
| O2 | 0.019(2) | 0.019(2) | 0.015(2) | 0.0026(17) | 0.0013(18) | 0.0007(18) |
| O3 | 0.013(2) | 0.017(2) | 0.016(2) | 0.0029(17) | -0.0007(17) | -0.0007(17) |
| O4 | 0.018(2) | 0.014(2) | 0.015(2) | -0.0016(16) | 0.0022(17) | 0.0026(17) |
| Oh5 | 0.014(2) | 0.0145(19) | 0.014(2) | 0.0005(16) | 0.0028(17) | -0.0013(16) |
| Oh6 | 0.017(2) | 0.0142(19) | 0.014(2) | -0.0030(17) | -0.0016(17) | -0.0030(17) |
| Oh7 | 0.015(2) | 0.015(2) | 0.017(2) | 0.0027(16) | 0.0034(18) | -0.0025(16) |
| Oh8 | 0.014(2) | 0.018(2) | 0.016(2) | -0.0023(17) | 0.0014(17) | 0.0000(16) |

and parallel, but offset strips *via* common OH6 atoms. Secondly, there are slightly twisted, finite chains of edge-sharing $\text{Mn}_2\text{O}_3(\text{OH})_3$ and $\text{Mn}_3\text{O}_3(\text{OH})_3$ octahedra, which run approximately parallel to $[\bar{1}02]$ and have a length comprising four octahedra (sequence Mn3–Mn2–Mn2–Mn3, Fig. 3). These chains of octahedra can be considered as fragments of infinite rutile-type chains. A single chain is corner-linked to four adjacent and parallel, but offset chains *via* common OH7 and OH8 atoms.

The unique PO_4 tetrahedron shares two of its neighboring edges with the Mn2- and Mn3-centered $\text{Mn}(\text{O},\text{OH})_6$ octahedra of the chains of octahedra mentioned (Figs. 3, 4). The fourth apex of the PO_4 tetrahedron is connected to the arsenoclasite-type strips of octahedra. Thus, PO_4 group provides a direct connection between the strips of octahedra and the chains of octahedra. The strongest bond-length distortions are shown by the Mn2- and Mn4-centered $\text{Mn}(\text{O},\text{OH})_6$ octahedra (*cf.* Table 5). The Mn2 atom in fact has a $[5 + 1]$ coordination to oxygen, and the Mn4 atom, a $[4 + 2]$ coordination. Average Mn–O bond lengths show values within an unexpectedly close range: 2.190 (Mn1) Å, 2.228 Å (Mn2), 2.228 Å (Mn3) and 2.235 Å (Mn4). The longer average Mn–O bond lengths for Mn(2), Mn(3) and Mn(4) are also reflected in the slightly low bond-valence sums for these atoms (Table 6).

In the PO_4 tetrahedron, the mean P–O bond length is 1.559 Å [range: 1.543(5) to 1.571(5) Å, Table 5], a value that is considerably longer than the grand mean P–O bond length observed in phosphates (1.537 Å; Baur 1981, Huminicki & Hawthorne 2002). This anomaly is explained, firstly, by the presence of small amounts of impurities on the P site (As, V, possibly Si; *cf.* Table 1), which all lead to an increased metal–oxygen distance and decrease the bond-valence sum (Table 6). A refinement of the occupancy of the P site gave an occupancy factor of 1.01, which indicates that the number of possible impurity elements at this site appears to be very small, however. A tentative P *versus* V refinement gave the occupancy ratio 0.984:0.016. Secondly, there is the already-mentioned fact that two of the four edges of the PO_4 tetrahedron are shared with the adjacent Mn2- and Mn3-centered $\text{Mn}(\text{O},\text{OH})_6$ octahedra (the edges O2–O4 and O1–O4, respectively, Fig. 4). As expected from the repulsion of the metal cations across the two shared edges, the Mn–O_{shared} and P–O_{shared} bond lengths are distinctly enlarged, with the exception of the P–O1 and P–O2 bonds (*cf.* Table 5). The oxygen atoms with the lowest bond-valence sums are O1, O2, and O4, which again reflects the fact that all three belong to the two shared edges of the PO_4 tetrahedron. In summary, geometric constraints lead to considerable distortion around the PO_4 tetrahedron.

RELATED COMPOUNDS AND CRYSTAL STRUCTURES

The fact that the PO_4 tetrahedron in waterhouseite shares two of its edges with $\text{Mn}(\text{O},\text{OH})_6$ octahedra is highly unusual. This feature of the crystal structure of waterhouseite is unique in the mineral kingdom. We are presently aware of only two (synthetic and anhydrous) arsenates in which an equivalent edge-sharing is present: $(\text{K}_4\text{Ni}_7(\text{AsO}_4)_6)$ (Ben Smail *et al.* 1999), and $\text{KNi}_3(\text{AsO}_4)(\text{As}_2\text{O}_7)$ (Ben Smail & Jouini 2000). Both of these arsenates contain fragments of brucite-type sheets of octahedra, and thus show some relation to waterhouseite.

There are several, mostly anhydrous phosphates and arsenates in which the XO_4 ($X = \text{P}, \text{As}$) tetrahedra share one of their edges with MO_6 ($M = \text{di- or trivalent metal}$) octahedra. The mineral representatives include gatehouseite, $\text{Mn}_5(\text{PO}_4)_2(\text{OH})_4$ (Pring & Birch 1993; see also Ruzsala *et al.* 1977) and the isotypic arsenoclasite, $\text{Mn}_5(\text{AsO}_4)_2(\text{OH})_4$ (Moore & Molin-Case 1971), which both also occur at the type locality of waterhouseite. Among the synthetic compounds, there are, for instance, $\text{K}_3\text{Fe}_2(\text{PO}_4)_3$ (Pintard-Scrépel *et al.* 1983), $\text{NaV}_3\text{P}_3\text{O}_{12}$ (Kinomura *et al.* 1989), $\text{K}_6\text{V}_2\text{P}_4\text{O}_{16}$ (Benhamada *et al.* 1991), $\text{K}_3\text{Fe}_3(\text{PO}_4)_4 \cdot \text{H}_2\text{O}$ (Lii 1995) and $\text{SrFe}_3(\text{PO}_4)_3$ (Korzanski *et al.* 1999).

Although the structure of waterhouseite is unique, Table 7 shows that the unit-cell parameters reveal some metric relations with the two chemical analogues allactite, $\text{Mn}_7(\text{AsO}_4)_2(\text{OH})_8$ (Moore 1968) and raadeite, $\text{Mg}_7(\text{PO}_4)_2(\text{OH})_8$ (Chopin *et al.* 2001). The latter two are isotypic, with space group $P2_1/n$. Unlike waterhouseite, they contain face-sharing MO_6 ($M: \text{Mn or Mg}$) octahedra, and the PO_4 tetrahedra in their frameworks are linked only *via* their corners, but not edges. It would seem interesting to synthesize further compounds with the general formula $M^{2+}_7(X^{5+}\text{O}_4)_2(\text{OH})_8$ in order to study their topology.

ACKNOWLEDGEMENTS

Glyn Francis kindly provided the specimens studied. David Beattie of the Ian Wark Research Institute, University of South Australia, is thanked for assistance with collecting the Raman spectra of waterhouseite. We also thank Drs F. Hatert, R.S.W. Braithwaite and A.-M. Franolet for their constructive reviews of the manuscript. The Alexander-von-Humboldt Foundation (Bonn, Germany) and the Australian Research Council are thanked for a Feodor–Lynen Fellowship to UK. A grant from the Mark Mitchell Foundation is also gratefully acknowledged.

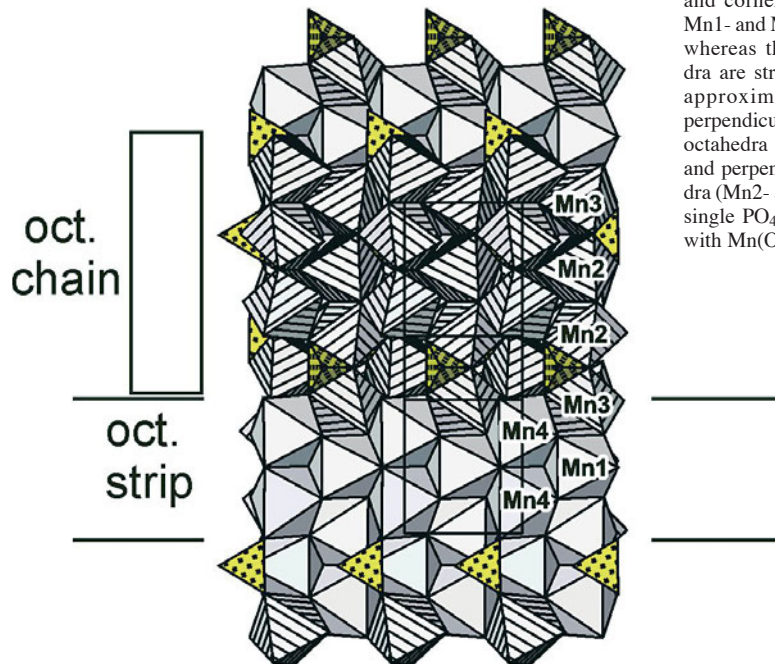
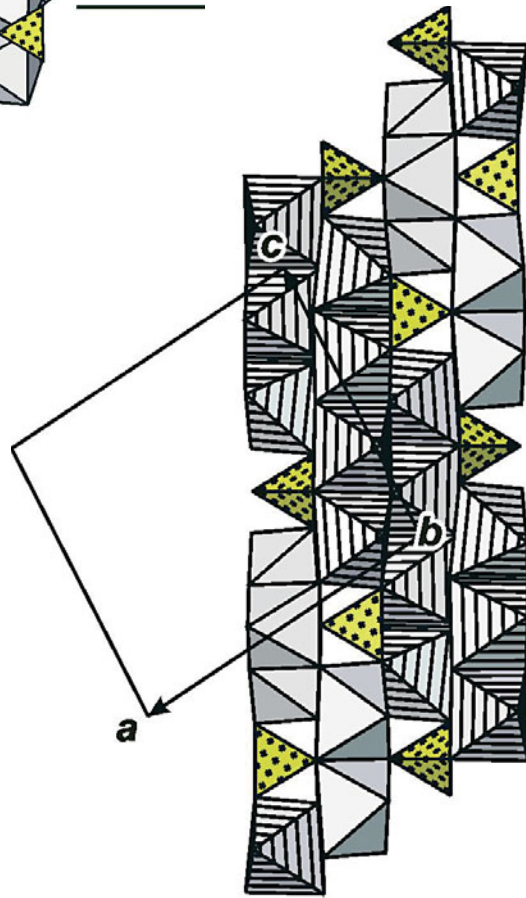


FIG. 3a. Polyhedral representation of the crystal structure of waterhouseite, ideally $\text{Mn}_7(\text{PO}_4)_2(\text{OH})_8$. The $\text{Mn}(\text{O},\text{OH})_6$ octahedra and PO_4 tetrahedra are linked by both edges and corners to form a dense framework. The Mn1- and Mn4-centered octahedra are unmarked, whereas the Mn2- and Mn3-centered octahedra are striped. The unit cell is outlined. View approximately along [201], approximately perpendicular to the arsenoclasite-type strips of octahedra (Mn1- and Mn4-centered octahedra) and perpendicular to the finite chains of octahedra (Mn2- and Mn3-centered octahedra); note the single PO_4 tetrahedron sharing two of its edges with $\text{Mn}(\text{O},\text{OH})_6$ octahedra (see also Fig. 3b).

FIG. 3b. Polyhedral representation of the crystal structure of waterhouseite, ideally $\text{Mn}_7(\text{PO}_4)_2(\text{OH})_8$. The $\text{Mn}(\text{O},\text{OH})_6$ octahedra and PO_4 tetrahedra are linked by both edges and corners to form a dense framework. The Mn1- and Mn4-centered octahedra are unmarked, whereas the Mn2- and Mn3-centered octahedra are striped. The unit cell is outlined. View along the *b* axis, parallel to the plane and elongation of the arsenoclasite-type strips of octahedra and perpendicular to the finite chains of octahedra. All structure drawings were done with ATOMS (Shape Software, 1999).



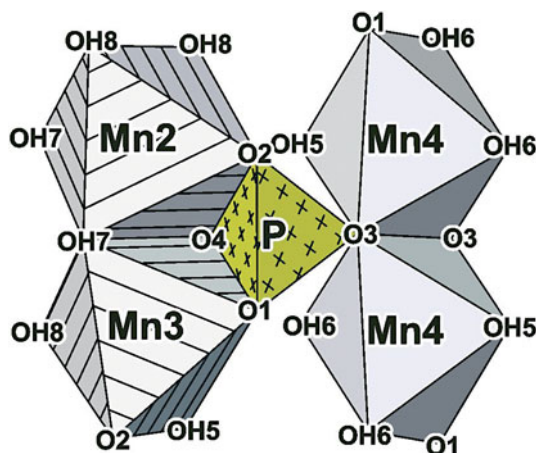


FIG. 4. Detailed view of bonding environment of the single PO_4 tetrahedron, which shares two of its edges with $\text{Mn}(\text{O},\text{OH})_6$ octahedra.

TABLE 5. SELECTED BOND-DISTANCES (Å) AND ANGLES (°) FOR THE COORDINATION POLYHEDRA IN WATERHOUSEITE

| | | | | | |
|----------|-----------------------------|----------|----------|------|----------|
| Mn1 | –O3 × 2 | 2.165(4) | Mn2 | –OH8 | 2.132(5) |
| | –OH6 × 2 | 2.178(4) | | –OH7 | 2.142(5) |
| | –OH5 × 2 | 2.226(5) | | –OH8 | 2.186(5) |
| <Mn1–O> | | 2.190 | | –OH7 | 2.189(5) |
| | | | | –O4 | 2.212(5) |
| | | | | –O2 | 2.507(5) |
| | | | <Mn2–O> | | 2.228 |
| Mn3 | –OH5 | 2.161(5) | Mn4 | –OH6 | 2.104(4) |
| | –O2 | 2.167(5) | | –OH6 | 2.127(4) |
| | –OH8 | 2.186(5) | | –OH5 | 2.132(5) |
| | –OH7 | 2.187(4) | | –O1 | 2.171(4) |
| | –O4 | 2.294(5) | | –O3 | 2.421(5) |
| | –O1 | 2.373(5) | | –O3 | 2.457(5) |
| <Mn3–O> | | 2.228 | <Mn4–O> | | 2.235 |
| P | –O1 | 1.543(5) | O1–P–O2 | | 112.3(3) |
| | –O2 | 1.554(5) | O1–P–O3 | | 112.2(3) |
| | –O3 | 1.567(5) | O2–P–O3 | | 111.8(3) |
| | –O4 | 1.571(5) | O1–P–O4 | | 105.2(2) |
| <P–O> | | 1.559 | O2–P–O4 | | 106.8(3) |
| | | | O3–P–O4 | | 108.1(2) |
| | | | <O–P–O> | | 109.4 |
| | Possible hydrogen bonds (Å) | | | | |
| OH5...O4 | | 3.12 | OH6...O3 | | 3.09 |
| OH6...O4 | | 2.90 | OH7...O2 | | 2.89 |

Note: OH8 does not seem to be involved in hydrogen bonding ($\text{OH8}\dots\text{O1} = 3.39 \text{ \AA}$).

REFERENCES

- BAUR, W.H. (1981): Interatomic distance predictions for computer simulation of crystal structures. *In* Structure and Bonding in Crystals II (M. O'Keefe & A. Navrotsky, eds.). Academic Press, New York, N.Y. (31–52).
- BEN SMAÏL, R., DRISS, A. & JOUINI, T. (1999): $\text{K}_4\text{Ni}_7(\text{AsO}_4)_6$. *Acta Crystallogr.* **C55**, 284–286.

TABLE 6. BOND-VALENCE ANALYSIS FOR WATERHOUSEITE

| | Mn1 | Mn2 | Mn3 | Mn4 | P | Sum* |
|------|-----------|--------------|-------|--------------|-------|------|
| O1 | | | 0.207 | 0.357 | 1.179 | 1.74 |
| O2 | | 0.144 | 0.361 | | 1.145 | 1.65 |
| O3 | 0.363 × 2 | | | 0.182, 0.165 | 1.105 | 1.82 |
| O4 | | 0.320 | 0.256 | | 1.093 | 1.67 |
| OH5 | 0.308 × 2 | | 0.367 | 0.397 | | 1.07 |
| OH6 | 0.350 × 2 | | | 0.428, 0.402 | | 1.18 |
| OH7 | | 0.340, 0.386 | 0.342 | | | 1.07 |
| OH8 | | 0.397, 0.343 | 0.343 | | | 1.08 |
| Sum* | 2.04 | 1.93 | 1.88 | 1.93 | 4.52 | |

Note: Bond-valence parameters used are from Brese & O'Keefe (1991).

* Sums (in valence units, vu) are derived from unrounded bond-valence contributions.

TABLE 7. COMPARISON OF WATERHOUSEITE WITH RELATED SPECIES

| Mineral | Waterhouseite | Raadeite | Allactite |
|--|---|--|---|
| Ref. | This work | Chopin <i>et al.</i> (2001) | Moore (1968) |
| Formula | $\text{Mn}_7(\text{PO}_4)_2(\text{OH})_8$ | $\text{Mg}_7(\text{PO}_4)_2(\text{OH})_8$ | $\text{Mn}_7(\text{AsO}_4)_2(\text{OH})_8$ |
| <i>a</i> (Å) | 11.364(6) | 5.250(1) | 5.51* |
| <i>b</i> (Å) | 5.570(2) | 11.647(2) | 12.12* |
| <i>c</i> (Å) | 10.455(3) | 9.655(2) | 10.12* |
| β (°) | 96.61(2) | 95.94(1) | 95.73* |
| <i>V</i> (Å ³) | 657.4(2) | 587.2 | 672.4 |
| Space group | $P2_1/c$ | $P2_1/n$ | $P2_1/n^*$ |
| <i>Z</i> | 2 | 2 | 2 |
| Strongest five lines in the powder pattern** | 3.619 (100) 4.415(70) 3.067(50) 2.940 (40) | 2.911(100) 2.202 (65) 3.142 (60) 3.554 (47) | 3.043 (100) 3.720 (54) 3.284 (48) 3.235 (44) |
| D(calc.) | 2.785(40) | 3.087 (41) | 2.902 (39) |
| Mohs hardness | ~4 | n.d. | 4.5 |
| α | 1.730(3) | 1.5945 | 1.755 |
| β | ~1.738 | 1.6069 | 1.772 |
| γ | 1.738(4) | 1.6088 | 1.774 |
| Birefringence | 0.008 | 0.014 | 0.019 |
| Optical character | (–) | (–) | (–) |
| Megascopic color | brownish | colorless | greenish, reddish***, pink, brownish grey |
| Habit | pseudo-orthorhombic | unknown (only in thin section) | pseudo-orthorhombic |
| Twinning | // to (100) | none | none |

* Reduced cell. The cell originally given (a 11.03, b 12.12, c 5.51 Å, β 114.1°; space group $P2_1/a$) is non-reduced.

** Calculated values are given for all minerals to avoid effects of preferred orientation.

*** Allactite may show an alexandrite effect (Nysten *et al.* 1999). n.d.: not determined.

& JOUINI, T. (2000): $\text{KNi}_3(\text{AsO}_4)(\text{As}_2\text{O}_7)$. *Acta Crystallogr.* **C56**, 513–514.

BENHAMADA, L., GRANDIN, A., BOREL, M.M., LECLAIRE, A. & RAVEAU, B. (1991): A new vanadium III potassium phosphate with a cage structure: $\text{K}_6\text{V}_2\text{P}_4\text{O}_{16}$. *J. Solid State Chem.* **91**, 264–270.

- BRESE, N.E. & O'KEEFFE, M. (1991): Bond-valence parameters for solids. *Acta Crystallogr.* **B47**, 192-197.
- CHOPIN, C., FERRARIS, G., PRENCIPE, M., BRUNET, F. & MEDENBACH, O. (2001): Raadeite, $Mg_7(PO_4)_2(OH)_8$: a new dense-packed phosphate from Modum (Norway). *Eur. J. Mineral.* **13**, 319-327.
- GELATO, L.M. & PARTHÉ, E. (1987): STRUCTURE TIDY – a computer program to standardize crystal structure data. *J. Appl. Crystallogr.* **20**, 139-143.
- HATERT, F., HERMANN, R.P., LONG, G.J., FRANSOLET, A.-M. & GRANDJEAN, F. (2003): An X-ray Rietveld, infrared and Mössbauer spectra study of the $NaMn(Fe_{1-x}In_x)_2(PO_4)_3$ alluaudite-type solid solution. *Am. Mineral.* **88**, 211-222.
- _____, REBOUGH, L., HERMANN, R.P., FRANSOLET, A.-M., LONG, G.J.V. & GRANDJEAN, F. (2005): Crystal chemistry of the hydrothermally synthesized $Na_2(Mn_{1-x}Fe^{2+}_x)_2Fe^{3+}(PO_4)_3$ alluaudite-like solid solution. *Am. Mineral.* **90**, in press.
- HUMINICKI, D.M.C. & HAWTHORNE, F.C. (2002): The crystal chemistry of the phosphate minerals. In *Phosphates – Geochemical, Geobiological, and Materials Importance* (M. J. Kohn, J. Rakovan & J.M. Hughes, eds.). *Rev. Mineral. Geochem.* **48**, 123-253.
- KINOMURA, N., MATSUI, N., KUMADA, N. & MUTO, F. (1989): Synthesis and crystal structure of $NaV_3P_3O_{12}$: a stuffed structure of α - $CrPO_4$. *J. Solid State Chem.* **79**, 232-237.
- KORZENSKI, M.B., KOLIS, J.W. & LONG, G.J. (1999): Hydrothermal synthesis, structural characterization, and physical properties of a new mixed valence iron phosphate, $SrFe_3(PO_4)_3$. *J. Solid State Chem.* **147**, 390-398.
- LE BAIL, A., DUROY, H. & FOURQUET, J.L. (1988): Ab-initio structure determination of $LiSbWO_6$ by X-ray powder diffraction. *Mater. Res. Bull.* **23**, 447-452.
- LIBOWITZKY, E. (1999): Correlation of O–H stretching frequencies and O–H...O hydrogen bond lengths in minerals. *Monatsh. Chem.* **130**, 1047-1059.
- LII, K.-H. (1995): $K_3Fe_3(PO_4)_4 \cdot H_2O$: an iron(III) phosphate with a layer structure. *Eur. J. Solid State Inorg. Chem.* **32**, 917-926.
- MILES, K.R. (1955): The geology and iron ore resources of the Middleback Range area. *Geol. Surv. S. Aust., Bull.* **33**.
- MANDARINO, J.A. (1981): The Gladstone–Dale relationship. IV. The compatibility concept and its application. *Can. Mineral.* **19**, 441-450.
- MOORE, P.B. (1968): Crystal chemistry of the basic manganese arsenate minerals. II. Crystal structure of allactite. *Am. Mineral.* **53**, 733-741.
- _____, & MOLIN-CASE, J. (1971): Crystal chemistry of the basic manganese arsenates. V. Mixed manganese coordination in the atomic arrangement of arsenoclasite. *Am. Mineral.* **56**, 1539-1552.
- NYSTEN, P., HOLTSTAM, D. & JONSSON, E. (1999): The Långban minerals. In *Långban – the Mines, their Minerals, Geology and Explorers* (D. Holtstam & J. Langhof, eds.). Swedish Museum of Natural History and Raster Förlag, Stockholm & C. Weise Verlag, Munich, Germany (89-183).
- OTWINOWSKI, Z., BOREK, D., MAJEWSKI, W. & MINOR, W. (2003): Multiparametric scaling of diffraction intensities. *Acta Crystallogr.* **A59**, 228-234.
- _____, & MINOR, W. (1997): Processing of X-ray diffraction data collected in oscillation mode. In *Methods in Enzymology*, v. **276**: *Macromolecular Crystallography A* (C.W. Carter, Jr. & R.M. Sweet, eds.). Academic Press, New York, N.Y. (307-326).
- PINTARD-SCRÉPEL, M., D'YVOIRE, F. & DURAND, J. (1983): Structure de l'tripotassium diiron(III) orthophosphate de difer(III) et de tripotassium, $K_3Fe_2(PO_4)_3$. *Acta Crystallogr.* **C39**, 9-12.
- PRING, A. & BIRCH, W.D. (1993): Gatehouseite, a new manganese hydroxy phosphate from Iron Monarch, South Australia. *Mineral. Mag.* **57**, 309-313.
- _____, FRANCIS, G.L. & BIRCH, W.D. (1989): Pyrobelonite, arsenoklasite, switzerite and other recent finds at Iron Monarch, South Australia. *Aust. Mineral.* **4**, 49-55.
- _____, _____ & _____ (1992a): Nissonite, namibite, and other additions to the mineral suite from Iron Monarch, South Australia. *Aust. Mineral.* **6**, 31-39.
- _____, GATEHOUSE, B.M. & BIRCH, W.D. (1990): Francisite, $Cu_3Bi(SeO_3)_2O_2Cl$, a new mineral from Iron Monarch, South Australia: description and crystal structure. *Am. Mineral.* **75**, 1421-1425.
- _____, KOLITSCH, U. & FRANCIS, G. (2000): Additions to the mineralogy of the Iron Monarch deposit, Middleback Ranges, South Australia. *Aust. J. Mineral.* **6**, 9-23.
- _____, SLADE, P.G. & BIRCH, W.D. (1992b): Shigaite from Iron Monarch, South Australia. *Mineral. Mag.* **56**, 417-419.
- RUSZALA, F.A., ANDERSON, J.B. & KOSTINER, E. (1977): Crystal structures of two isomorphs of arsenoclasite: $Co_5(PO_4)_2(OH)_4$ and $Mn_5(PO_4)_2(OH)_4$. *Inorg. Chem.* **16**, 2417-2422.
- SHAPE SOFTWARE (1999): ATOMS for Windows and Macintosh V5.0.4. Kingsport, Tennessee 37663, U.S.A.
- SHELDRIK, G.M. (1997a): SHELXS-97, a Program for the Solution of Crystal Structures. University of Göttingen, Göttingen, Germany.
- _____, (1997b): SHELXL-97, a Program for Crystal Structure Refinement. University of Göttingen, Göttingen, Germany.
- WAVEMETRICS INC. (2000): IGOR PRO version 4.0. WaveMetrics Inc., Lake Oswego, Oregon.
- YEATES, G. (1990): Middleback Range iron ore deposits. In *Geology of the Mineral Deposits of Australia and Papua New Guinea* (F.E. Hughes, ed.). The Australasian Institute of Mining and Metallurgy, Melbourne, Australia (1045-1048).

Received January 17, 2005, revised manuscript accepted July 31, 2005.